International Journal of Peptide Research and Therapeutics (2023) 29:73
https://doi.org/10.1007/s10989-023-10548-9

The Nuclear Localization Signal of NF-κB p50 Enters the Cells via Syndecan-Mediated Endocytosis and Inhibits NF-κB Activity

Annamária Letoha[1] · Anett Hudák[2] · Zsolt Bozsó[3] · Csaba Vizler[4] · Gábor Veres[2] · László Szilák[2] · Tamás Letoha[2]

Accepted: 22 June 2023

Abstract
It is well established that cationic peptides can enter cells following attachment to polyanionic membrane components. We report that the basic nuclear localization signal (NLS) of the NF-κB p50 subunit is internalized via lipid raft-dependent endocytosis mediated by heparan sulfate proteoglycans and exerts significant NF-κB inhibitory activities both in vitro and in vivo. In vitro uptake experiments revealed that the p50 NLS peptide (CYVQRKRQKLMP) enters the cytoplasm and accumulates in the nucleus at 37 °C. Depleting cellular ATP pools or decreasing temperature to 4 °C abolished peptide internalization, confirming the active, energy-dependent endocytic uptake. Co-incubation with heparan sulfate or replacing the peptide's basic residues with glycines markedly reduced the intracellular entry of the p50 NLS, referring to the role of polyanionic cell-surface proteoglycans in internalization. Furthermore, treatment with methyl-β-cyclodextrin greatly inhibited the peptide's membrane translocation. Overexpression of the isoforms of the syndecan family of transmembrane proteoglycans, especially syndecan-4, increased the cellular internalization of the NLS, suggesting syndecans' involvement in the peptide's cellular uptake. In vitro, p50 NLS reduced NF-κB activity in TNF-α-induced L929 fibroblasts and LPS-stimulated RAW 264.7 macrophages. TNF-α-induced ICAM-1 expression of HMEC-1 human endothelial cells could also be inhibited by the peptide. Fifteen minutes after its intraperitoneal injection, the peptide rapidly entered the cells of the pancreas, an organ with marked syndecan-4 expression. In an acute pancreatitis model, an inflammatory disorder triggered by the activation of stress-responsive transcription factors like NF-κB, administration of the p50 NLS peptide reduced the severity of pancreatic inflammation by blocking NF-κB transcription activity and ameliorating the examined laboratory and histological markers of pancreatitis.

Keywords NF-κB · Nuclear localization signal peptide · Peptide transduction · Endocytosis · Syndecan · Pancreatitis

Introduction

Peptide-mediated import of biomolecules has become a popular approach to modulating cellular functions (Heitz et al. 2009; Bohmova et al. 2018; Sanchez-Navarro 2021; Shoari et al. 2021; Yokoo et al. 2021;). Efficient intracellular delivery of bioactive compounds (peptides, oligonucleotides, etc.) with cell-penetrating peptides (CPPs)—small cationic peptides readily translocating through cell membranes and delivering attached cargoes intracellularly—opened up new possibilities for therapeutic interventions (Dougherty et al. 2019; Xie et al. 2020; Liu et al. 2021; Tarvirdipour et al. 2021). At the time of CPP discovery, endocytosis—due to lysosomal degradation of internalized agents—was viewed as an entry mechanism to be avoided for the intracellular delivery of bioactive agents. Thus, early studies claimed endocytosis-independent cellular internalization of CPPs (Derossi et al. 1994, 1996, 1998; Oehlke et al. 1997; Vives et al. 1997; Letoha et al. 2003). However, the broadening knowledge of the newly explored lipid raft- and caveolae-mediated endocytic pathways helped to redefine the molecular mechanism of CPPs' efficient cellular

✉ Tamás Letoha
tamas.letoha@pharmacoidea.eu

1 Department of Medicine, Albert Szent-Györgyi Clinical Center, Faculty of Medicine, University of Szeged, Szeged 6720, Hungary

2 Pharmacoidea Ltd., Szeged 6726, Hungary

3 Department of Medical Chemistry, Albert Szent-Györgyi Medical School, University of Szeged, Szeged 6720, Hungary

4 Institute of Biochemistry, Biological Research Centre, Szeged 6726, Hungary

Published online: 05 July 2023

entry and avoidance of lysosomal degradation (Nichols and Lippincott-Schwartz 2001; Nichols 2003; Parton and Richards 2003; Bathori et al. 2004; Kirkham and Parton 2005). Due to the advances in endocytosis research, later studies clearly showed that contrary to earlier claims, CPPs utilize endocytic pathways to transport attached cargoes into the cells (Console et al. 2003; Drin et al. 2003; Fittipaldi et al. 2003; Richard et al. 2003). These newer studies confirmed that contrary to early anti-endocytic hypotheses, specific endocytic pathways can be efficiently exploited to deliver biomolecules into the cells (LeCher et al. 2017).

One of the earliest CPPs was a conjugate of the hydrophobic domain of Kaposi's sarcoma fibroblast growth factor signal sequence and the NLS of NF-κB p50 that can enter the cells and block the nuclear import of stress-responsive transcription factors (SRTFs) like NF-κB, AP-1, STAT1, and NFAT in inflammatory conditions (Lin et al. 1995; Torgerson et al. 1998; Zhang et al. 1998; Kolenko et al. 1999; Liu et al. 2000; Letoha et al. 2005a, b, c). This NF-κB NLS-containing conjugate named SN50 was claimed to be internalized via an endocytosis/receptor-independent mechanism (Veach et al. 2004). Cellular internalization was attributed purely to the hydrophobic signal sequence, while the basic NF-κB p50 NLS peptide alone was thought to be non-cell-permeable and thus have no biological effects (Torgerson et al. 1998). The wild-type (WT) NF-κB p50 NLS peptide (CYVQRKRQKLMP) specifically interacts with the cytoplasmic Rch1/importin-β NLS receptor complex of Jurkat cell extracts, but it was reasoned that without the hydrophobic signal sequence this cationic NLS was unable to enter the cells and inhibit the inducible nuclear import of NF-κB proteins (including p50 and p65) and other SRTFs (Torgerson et al. 1998; Boothby 2001). This reasoning seemed inconsistent with the advanced concepts of cationic peptide internalization. As described above, cationic peptides have been widely used to import bioactive cargoes intracellularly, and basic NLS peptides can even transport DNA into the nucleus (Eguchi et al. 2001; Snyder and Dowdy 2001; Akuta et al. 2002; Nakanishi et al. 2003; Arenal et al. 2004; Ahmed 2017; Vedadghavami et al. 2020). Ragin et al. demonstrated that the NLS of the NF-κB p50 subunit is also internalized by cells at 37 °C and facilitates intracellular delivery of attached compounds (Ragin et al. 2002; Ragin and Chmielewski 2004). It is widely established that peptides abundant in arginines and lysines have the unique character to be taken up by cells through endocytic pathways induced by electrostatic binding to polyanionic proteoglycans (Sandgren et al. 2002; Belting 2003; Futaki et al. 2007; Poon and Gariepy 2007; Christianson and Belting 2014; Zhu and Jin 2018). Previously we demonstrated the syndecan-dependent cellular uptake of cationic CPPs (Letoha et al. 2010). Syndecans (SDCs), a family of transmembrane heparan-sulfate proteoglycans (HSPGs), efficiently deliver a wide range of ligands intracellularly by attaching them through their versatile polyanionic heparan-sulfate (HS) sidechains (Christianson and Belting 2014; Afratis et al. 2017). Microbes, growth factors, and other endogenous proteins endowed with cationic heparin-binding sequences can attach to SDCs and enter the cells via SDC-mediated endocytosis (Gallay 2004; Elfenbein and Simons 2013; Favretto et al. 2014; Cagno et al. 2019; Hudak et al. 2019; Letoha et al. 2019; Stow et al. 2020; De Pasquale et al. 2021; Hudak et al. 2021a, b, 2022).

Considering the immense evidence on the HSPG-mediated uptake of cationic peptides, we reexamined the cellular internalization and biological activity of the cationic NF-κB p50 NLS unconjugated to any translocating peptide sequence. The peptide was labeled with FITC, and its uptake was investigated in vitro and in vivo. Besides general cell uptake studies, the NLS' internalization was also assessed in SDC-specific cellular assays. Effects of the peptide on NF-κB transcriptional activity were analyzed with various in vitro inflammatory models, including NF-κB reporter gene assays enabling the quantitative assessment of inducible NF-κB activity based on luminescence (Letoha et al. 2005a, b, c; Letoha et al. 2006). The NF-κB inhibitory activity of the peptide was tested in vivo in an experimental model of acute pancreatitis, an inflammatory disorder initiated by the activation of SRTFs, including NF-κB and AP-1 (Gukovsky et al. 2003; Letoha et al. 2005a, b, c, 2006, 2007; Gukovsky and Gukovskaya 2013; Yu and Kim 2014). Since activated NF-κB is one of the most significant initiators of pancreatic inflammation, CCK-induced acute pancreatitis offered an ideal experimental model to monitor the efficacy of the p50 NLS in inhibiting NF-κB activity in vivo (Gukovsky et al. 1998; Williams et al. 2002; Letoha et al. 2005a, b, c, 2006, 2007; Gukovsky and Gukovskaya 2013; Huang et al. 2013). The broad inhibitory spectrum of the p50 NLS on NF-κB proteins (i.e., p50 NLS competes for proteins generally involved in nuclear import of NF-κB proteins, including p50 and p65) seemed also beneficial in the complex NF-κB activation pathway of pancreatitis (Boothby 2001; Gukovsky and Gukovskaya 2013; Huang et al. 2013).

Our results confirm that HSPG-, particularly SDC-mediated endocytosis can be utilized for efficient peptide transduction in vitro and in vivo. Thus, the present manuscript undermines the receptor-independent, non-endocytic uptake of the cationic NLS peptide and marks new pathways to be utilized for the intracellular delivery of novel bioactive, cationic peptides.

Results

The NF-κB p50 NLS is Internalized by Live, Unfixed Cells

Confocal microscopic experiments on NF-κB p50 NLS-treated live, unfixed cells (HMEC-1 human microvascular

endothelial cells, L929 murine fibroblasts, and RAW 264.7 murine macrophages) showed a gradual increase in fluorescence following the addition of the FITC-labeled NLS peptide at a concentration of 20 µM at 37 °C (Fig. 1). Intracellular fluorescence increased markedly at 30 min of incubation, demonstrating efficient internalization. At 90 min the FITC-labeled p50 NLS peptide appeared in the nuclei where it accumulated. Adding the NLS peptide to cells at 4 °C, a temperature where the rigidity of cellular membranes unable endocytosis, hindered the cellular entry of the peptide, hence demonstrating the endocytic nature of uptake (Supplementary Fig. S1). Replacing the basic residues with glycines (i.e., CYVQGGGQGLMP, indicated as GlyNLS) also impeded cellular uptake of the NLS, as intracellular fluorescence of cells treated with the FITC-labeled GlyNLS analog remained almost undetectably low even at 90 min of incubation at 37 °C, hence demonstrating the lack of uptake due to the loss of the basic residues (Supplementary Fig. S1). Simultaneous cell viability studies showed that neither the NLS nor its Gly analog (GlyNLS) affected cellular viability from concentrations of 1.56 µM to 50 µM (Supplementary Fig. S2).

Flow Cytometric Assessment of the NF-κB p50 NLS

Cellular uptake of the FITC-labeled p50 NLS peptide (NLS; at a concentration of 20 µM) was then quantified with standard flow cytometry. Fluorescence of surface-bound peptides was quenched by adding trypan blue (at a concentration of 0.25% in ice-cold 0.1 M citrate buffer pH 4.0) one minute before flow cytometry hence only the intracellular FITC-labeled NLS was measured (Letoha et al. 2010, 2019). After 30 min of incubation, a small increase in the cellular fluorescence of the NLS-treated cells could be detected at 37 °C (Fig. 2a). At 60 and 90 min, intracellular fluorescence further increased, especially in RAW macrophages (Fig. 2b, c). ATP-depletion (with 0.1% mM sodium azide and 50 mM 2-deoxy-D-glucose) resulted in low intracellular fluorescence, which showed diminished peptide uptake (Fig. 2a–c). Pretreating the cells with methyl-β-cyclodextrin (MCD) to remove cholesterol from the membrane markedly reduced intracellular fluorescence, suggesting the involvement of the cholesterol-enriched lipid rafts in the cellular internalization of the peptide at 37 °C (Fig. 2a–c). Exogenous heparan-sulfate (HS; 25 µg/mL) also diminished intracellular fluorescence at 37 °C, indicating the involvement of polyanionic surface proteoglycans in attaching the cationic peptide (Fig. 2a–c). At 4 °C the cellular membranes become extremely rigid which stops endocytosis. At 4 °C all cells treated with the FITC-labeled peptide exhibited very low cellular fluorescence, providing further evidence of the endocytic nature of NLS uptake (Fig. 2d).

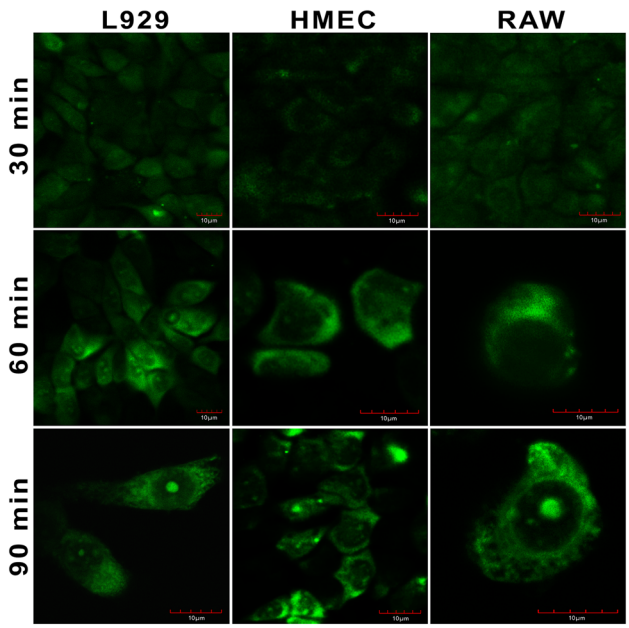

Fig. 1 Cellular internalization of the NF-κB p50 NLS visualized with confocal microscopy. HMEC-1, L929, and RAW 264.7 cells were treated with the FITC-labeled NF-κB p50 NLS for 30, 60, and 90 min at a concentration of 20 µM at 37 °C. Peptide uptake was examined with confocal microscopy. Scale bar = 10 µm

SDCs Mediate the Cellular Internalization of the NF-κB p50 NLS

The contribution of SDCs to several cationic CPPs have already been explored (Letoha et al. 2010; Montrose et al. 2013). Considering the previously obtained data on the HS-dependent uptake of the NLS, we studied its uptake in cell lines expressing specific SDC isoforms. K562 cells reportedly exhibit very low endogenous HSPG expression, except for a minimal amount of betaglycan and SDC3 (Shafti-Keramat et al. 2003; Letoha et al. 2010). Due to their low HSPG expression and lack of caveolin-1, the molecular base of caveolae-mediated endocytosis, K562 cells offer an ideal cellular environment to express SDC isoforms and study their functionality without the interference of other HSPGs and caveolae-mediated endocytosis (Parolini et al. 1999; Hudak et al. 2019; Letoha et al. 2019). After creating stable SDC transfectants in K562 cells, the various SDC-expressing clones were selected and standardized according to their HS expression (Supplementary Fig. S3) (Hudak et al. 2019, 2021b, 2022; Letoha et al. 2019). Thus stable SDC transfectants with even HS expression were selected and, along with WT K562 cells, incubated with the FITC-labeled NLS peptide for 90 min at 37 °C. Cellular internalization of the fluorescently labeled NLS was assessed with imaging flow cytometry. To remove surface fluorescence due to extracellularly attached fluorescent NLS, peptide-treated cells were

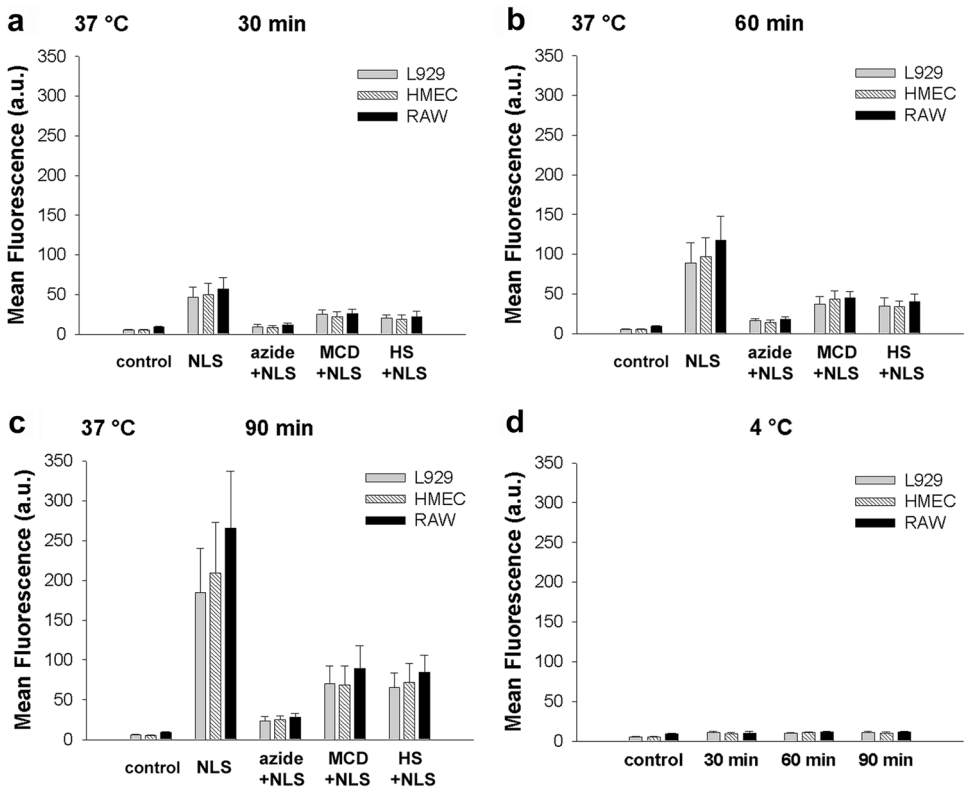

Fig. 2 Cellular internalization of the NF-κB p50 NLS peptide quantified with flow cytometry. HMEC-1, L929, and RAW 264.7 cells were treated with the FITC-labeled p50 NLS peptide ("NLS") at a concentration of 20 μM for various amounts of time and cellular fluorescence was analyzed with FACS. ATP-depletion was carried out by incubating the cells with 0.1% sodium azide ("azide") and 50 mM 2-deoxy-D-glucose in Opti-MEM for 60 min prior to the addition of the NLS peptide at 37 °C. To disrupt lipid rafts, some of the cells were treated with 5 mM/mL of MCD for 60 min before peptide treatment. Other cells were co-incubated with 25 μg/mL of heparan sulfate (HS) and the NLS peptide. **a–c** show the results of the flow cytometric analyses at 37 °C and **d** shows the ones at 4 °C. The bars represent the mean + SEM of four independent experiments. a.u., arbitrary units

trypsinized with the method of Nakase et al. before the flow cytometric analyses (Nakase et al. 2007; Hudak et al. 2019, 2021b, 2022). Imaging flow cytometry demonstrated that SDC overexpression increases NLS uptake, especially SDC4, that increased cellular uptake of the FITC-labeled NLS the most (Fig. 3a–c). Simultaneous cell viability measurements showed that the NLS did not affect cellular viability at the applied concentrations of 20 μM (Supplementary Fig. S4).

The NF-κB p50 NLS Peptide Suppresses NF-κB Transcription Activity in Different Cell Types

Luciferase reporter gene assays, utilizing stably transformed cells expressing the firefly luciferase under NF-κB-responsive elements, were used next to study the in vitro NF-κB inhibitory effects of the NF-κB p50 NLS peptide. The proinflammatory cytokine TNF-α (10 U/mL) induces NF-κB-driven luciferase activity in L929 cells (Fig. 4a). Treatment with the NF-κB p50 NLS 30 min prior to TNF-α dose-dependently and markedly reduced TNF-α–induced NF-κB activity at concentrations between 1.56 and 25 μM (Fig. 4a).

The NF-κB inhibitory effect of the peptide was then measured in LPS-stimulated murine macrophages. The p50 NLS decreased the LPS-induced luciferase activity of RAW 264.7 macrophages, however, to a smaller extent than in the case of TNF-α-induced L929 fibroblasts (Fig. 4b).

TNF-α induces ICAM-1 expression on the surface of HMEC-1 cells through NF-κB-dependent mechanisms (True et al. 2000). As shown in Fig. 5c, NF-κB-dependent ICAM-1 expression was reduced by NF-κB p50 NLS pretreatment (Fig. 4c). Replacing the basic residues of the NLS with glycines abolished the peptide's inhibitory effect on NF-κB or ICAM-1 expression, demonstrating that cationic residues and efficient internalization is crucial for the peptide's bioactivity (Supplementary Fig. S5).

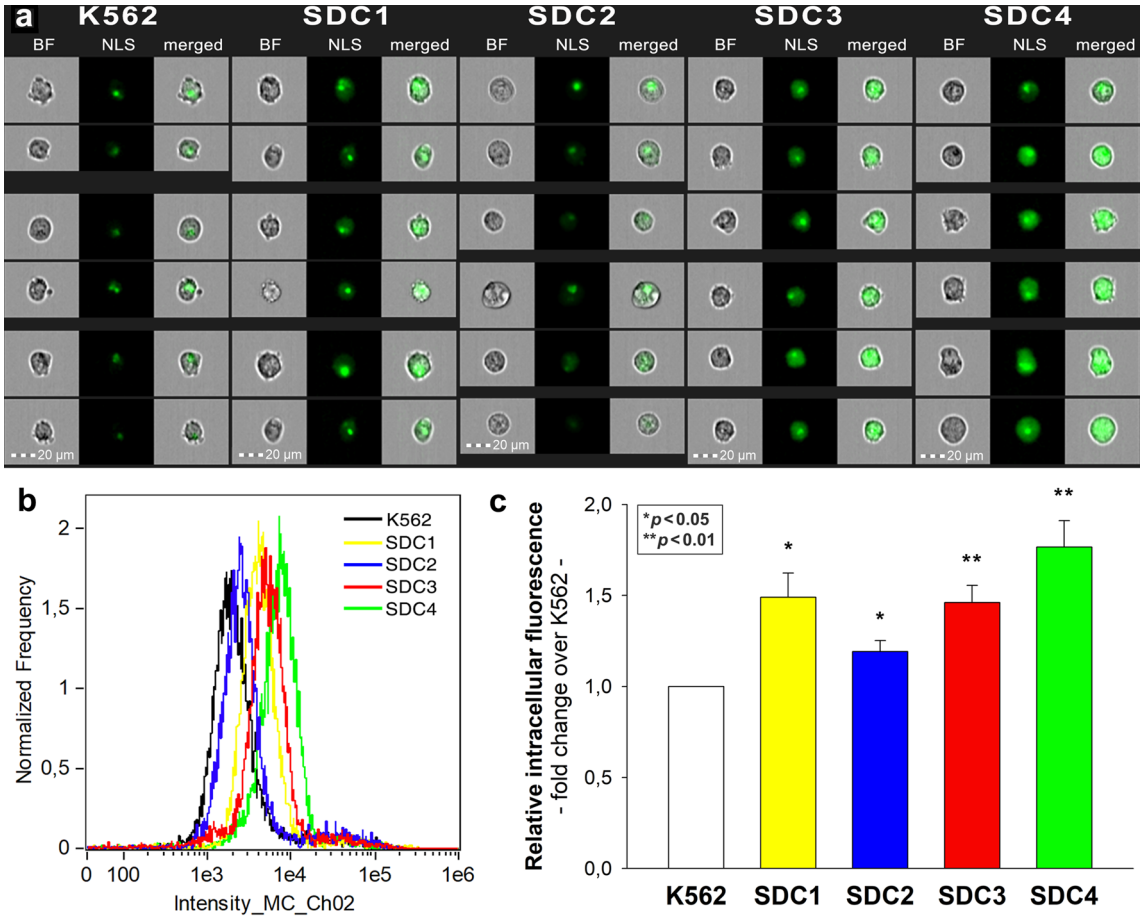

Fig. 3 SDC isoforms enhance the in vitro cellular uptake of the NF-κB p50 NLS. WT K562 cells and SDC transfectants were treated with the FITC-labeled NLS at a concentration of 20 µM for 90 min at 37 °C. After incubation, the cells were washed, trypsinized and cellular uptake was evaluated with imaging flow cytometry. **a** Brightfield (BF) and fluorescent cellular images of FITC-NLS-treated WT K562 cells and SDC transfectants. Scale bar = 20 µm. **b** Representative flow cytometry histograms showing the intracellular fluorescence of FITC-NLS-treated WT K562 cells and SDC transfectants. **c** Detected fluorescence intensities were normalized to FITC-NLS-treated WT K562 cells as standards. The bars represent the mean + SEM of four independent experiments. Statistical significance vs. standards was assessed with analysis of variance (ANOVA). *$p < 0.05$; **$p < 0.01$

The NF-κB p50 NLS Peptide Ameliorates Acute Experimental Pancreatitis

After demonstrating the efficient intracellular uptake and the NF-κB suppressing the activity of the p50 NLS in vitro, we tested the peptide's anti-inflammatory effects in an animal model of acute pancreatitis, a disease triggered by activated SRTFs including NF-κB.

First, we analyzed whether the peptide could enter the pancreas in vivo. According to the Human Protein Atlas, the pancreas shows a definite SDC4 expression (Uhlen et al. 2005, 2015). Thus, pancreas tissues were dissected from rats 15 min after intraperitoneal (IP) injection of the FITC-labeled p50 NLS peptide or pure PBS (controls). Fluorescent microscopic analysis revealed fluorescent intracellular signals, the characteristic features of endocytosis in the pancreatic samples of the NLS-injected rats (Fig. 5b, c), demonstrating that the NF-κB p50 NLS peptide was internalized in vivo. Contrary to the NLS-injected rats, the pancreas of control animals displayed low and blunt autofluorescence without any distinct intracellular signs of endocytosis (Fig. 5a–c). Cellular uptake studies also showed the efficient cellular entry of the fluorescently labelled p50 NLS peptide into AR42J pancreatic acinar cells (Supplementary Fig. S6). Unlike the p50 NLS peptide, the GlyNLS analog in which the basic residues are replaced with glycines (i.e., CYVQGGGQGLMP) exhibited no sign of cellular uptake into AR42J cells.

After showing its efficient in vivo delivery into the pancreas, the NLS' effects were studied in the experimental model of CCK-induced pancreatitis. Rats receiving 2 × 100 µg/kg body weight of CCK IP exhibited the relevant molecular and histological features of pancreatic inflammation, including intrapancreatic edema and cellular damage

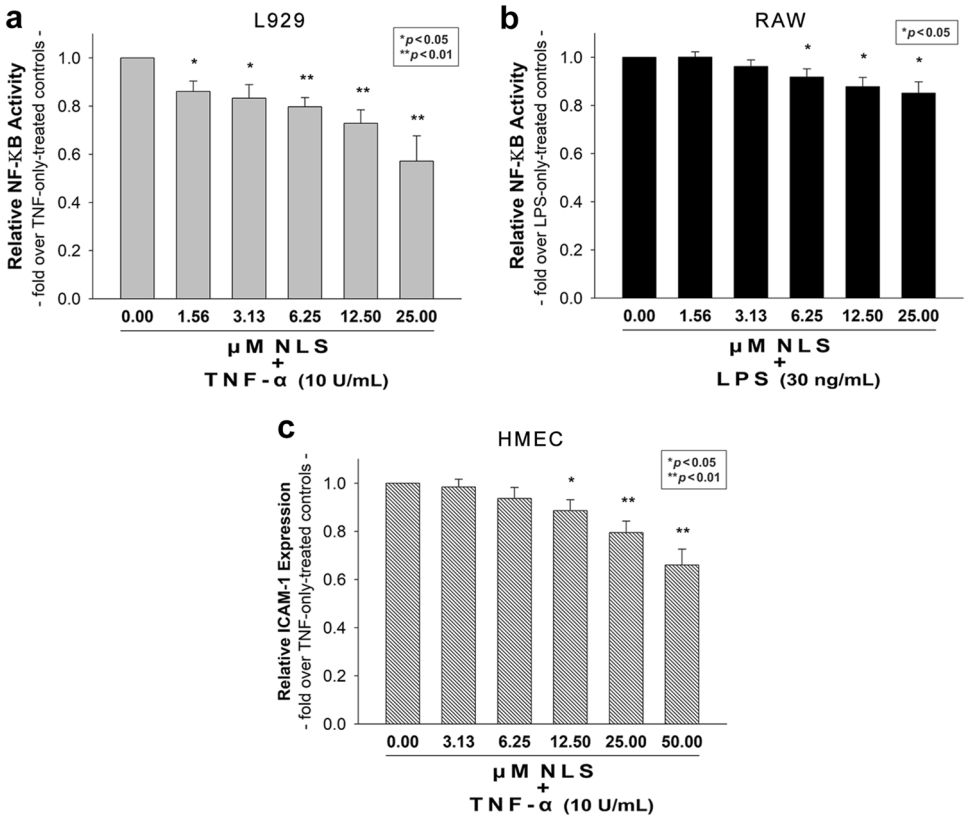

Fig. 4 TNF-α–induced NF-κB transcriptional activity and ICAM-1 expression is suppressed by the NF-κB p50 NLS suppresses in vitro. **a**, **b** Luciferase reporter assays of TNF-α-triggered L929 fibroblasts (**a**) and LPS-activated RAW 264.7 macrophages (**b**) with NF-κB-Luc are shown. Controls were treated with 10 U/mL of TNF-α or 30 ng/mL LPS. The p50 NLS-treated cells were incubated with various peptide concentrations for 30 min before 10 U/mL TNF-α or 30 ng/mL LPS was added. Luciferase activity was analyzed 6 h later. Detected luminescence intensities were normalized to TNF-α or LPS-only-treated cells as standards. The bars represent the means + SEM of four independent experiments. **c** Surface ICAM-1 expression as detected with flow cytometry on HMEC-1 cells pretreated with the p50 NLS for 30 min before TNF-α (10 U/mL) incubation for 6 h. Detected ICAM-1 expression values were normalized to TNF-α-only-treated cells as standards. The bars represent the means + SEM of four independent experiments

(as revealed by the increased pancreatic weight/body weight ratio and serum amylase activity in Fig. 6a). Concentrations of proinflammatory cytokines, TNF-α and IL-6 in the pancreas were also significantly increased (Fig. 6b). Supramaximal CCK doses triggered leukocyte sequestration, raising MPO activities in the pancreas and the lung (Fig. 6c). CCK also induced ROS production. Thus the level of MDA, the measure of lipid peroxidation, was significantly higher compared to controls. Due to increased ROS production, intrapancreatic GSH (that participates in eliminating ROS) was depleted after two injections of CCK (Fig. 6d). Pretreatment with 2 mg/kg of the NF-κB p50 NLS peptide IP 30 min before the first CCK dose improved all these laboratory parameters, thus ameliorating the pancreatitis-inducing effects of CCK (Fig. 6a–d).

Electrophoretic mobility shift assay (EMSA) performed on nuclear extracts of pancreas samples was utilized to assess the NF-κB inhibitory effect of the peptide. The DNA-binding activity of NF-κB was relatively weak in the untreated controls (Fig. 7). CCK administration significantly increased the DNA-binding activity of NF-κB, which could be inhibited with the p50 NLS pretreatment. While CCK also induced the degradation of IκB-α, pretreatment with the p50 NLS peptide had no significant effect on CCK-induced degradation of IκB-α (Supplementary Fig. S7).

Histology revealed that administration of 2 × 100 μg/kg body weight CCK induced acute pancreatitis, which was characterized by microfocal necrosis, vacuolar degeneration, marked edema, inflammatory activity, and stasis (Fig. 8a). Pretreatment with 2 mg/kg of the NF-κB p50 NLS peptide significantly reduced the morphological damage induced by CCK in the pancreas (Fig. 8b). The values for each of the scored parameters are shown in Table 1.

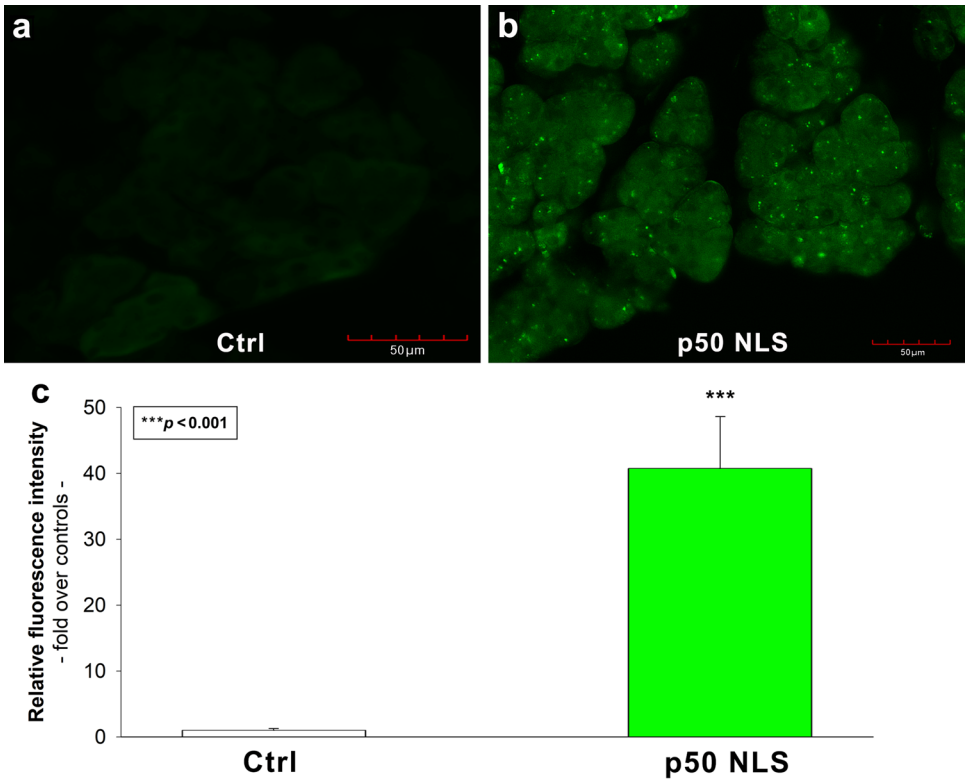

Fig. 5 The pancreas internalizes the NF-κB p50 NLS in vivo. The in vivo internalization studies were carried out by injecting 20 nM/kg body weight of FITC-labeled NF-κB p50 NLS or PBS (Ctrl) IP into male Wistar rats. The images show pancreas samples taken from rats 15 min after injecting PBS (**a**) or the FITC-labeled NLS peptide (**b**) IP. Images represent three independent studies. Scale bar = 50 µm. **c** BioTek Gen5 Software was utilized to assess fluorescence intensity of pancreatic samples. Two samples from each group from three independent studies were analyzed. Detected fluorescence intensities were normalized to PBS-treated controls. The bars represent the mean + SEM of six samples from three independent experiments. Statistical significance vs. Ctrl was assessed with ANOVA. ***$p < 0.001$

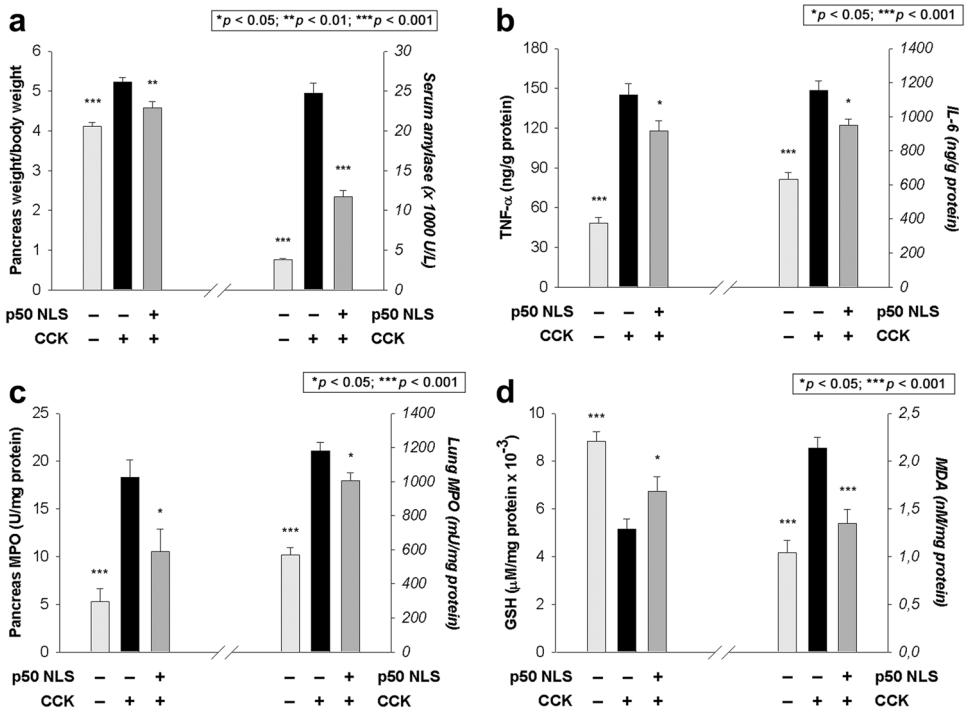

Fig. 6 The NF-κB p50 NLS peptide improves the laboratory markers of acute pancreatitis in vivo. Acute pancreatitis was induced with 2 × 100 µg/kg of CCK IP in male Wistar rats. p50 NLS peptide-treated animals received 2 mg/kg IP of the p50 NLS 30 min before the first CCK dose. Figure **a** shows pancreatic weight/body weight ratio and serum amylase activity, **b** shows intrapancreatic TNF-α and IL-6 levels, **c** shows pancreatic and lung MPO activity and **d** shows pancreatic MDA and GSH levels. Means + SEM of 10 animals in each group are shown. Light gray bars represent controls (receiving 3 × 0.5 mL of PBS IP), black bars represent Group CCK (animals receiving 2 × 100 µg/kg of CCK IP) and dark gray bars represent Group NLS + CCK (animals treated with 2 mg/kg of p50 NLS IP 30 min before the first injection of CCK). *$p < 0.05$ vs Group CCK; **$p < 0.01$ vs Group CCK

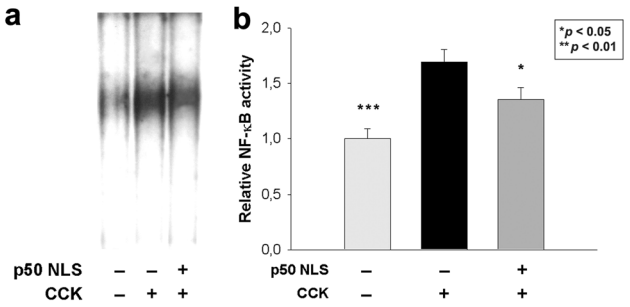

Fig. 7 The NF-κB p50 NLS peptide inhibits NF-κB transcription activity in acute pancreatitis in vivo. **a** A representative EMSA showing DNA-binding activity of NF-κB in pancreatic samples. **b** Intensities of NF-κB bands were densitometrically quantified relative to untreated controls (i.e., normal pancreas). Values presented are means + SEM, n = 10 animals/group. Light gray bars represent controls (receiving 3 × 0.5 mL PBS IP), black bars represent Group CCK (animals receiving 2 × 100 µg/kg of CCK IP) and dark gray bars represent Group NLS + CCK (animals treated with 2 mg/kg of p50 NLS IP 30 min before the first injection of CCK). *$p < 0.05$ vs Group CCK; **$p < 0.01$ vs Group CCK

Discussion

As proteoglycan-mediated endocytic uptake of cationic peptides is now widely established, it is time to reconsider our views about the internalization of biomolecules. Our study demonstrates that basic nuclear localization signal (NLS) of the NF-κB p50 subunit—without any cell-transporter motif attached—can be efficiently internalized through proteoglycan-mediated endocytic pathways and retain its reported biological activity to inhibit NF-κB's nuclear translocation and transcriptional activity.

Considering current knowledge on proteoglycan-mediated peptide transduction, it is unsurprising that a cationic 12-mer NLS peptide can enter the cells via endocytosis. Endocytosis is a complex mechanism that involves clathrin-dependent and independent pathways (Kumari et al. 2010). Clathrin-independent endocytosis includes phagocytosis, constitutive pinocytotic pathways, and endocytosis mediated by caveolae and glycolipid rafts (Nichols and Lippincott-Schwartz 2001; Nichols 2003; Parton and Richards 2003; Kirkham and Parton 2005). Contrary to classic clathrin-dependent endocytosis, caveolar or lipid raft-mediated internalization can avoid the lysosomes and hence the degradation of internalized molecules (Bathori et al. 2004; Kiss and Botos 2009; Sousa de Almeida et al. 2021). As recycling and internalization of proteoglycans occur through lipid rafts, thus by attaching to polyanionic cell surface proteoglycans, cationic peptides can utilize lipid raft-mediated pathways to enter the cells (Belting 2003; Christianson and Belting 2014). The importance of binding to polyanionic heparan sulfate proteoglycans and entering the cells by lipid-raft-mediated endocytosis was clearly confirmed in our flow cytometric uptake experiments when incubating the cells with HS or MCD markedly decreased internalization of the NLS peptide. The replacement of basic residues with glycine

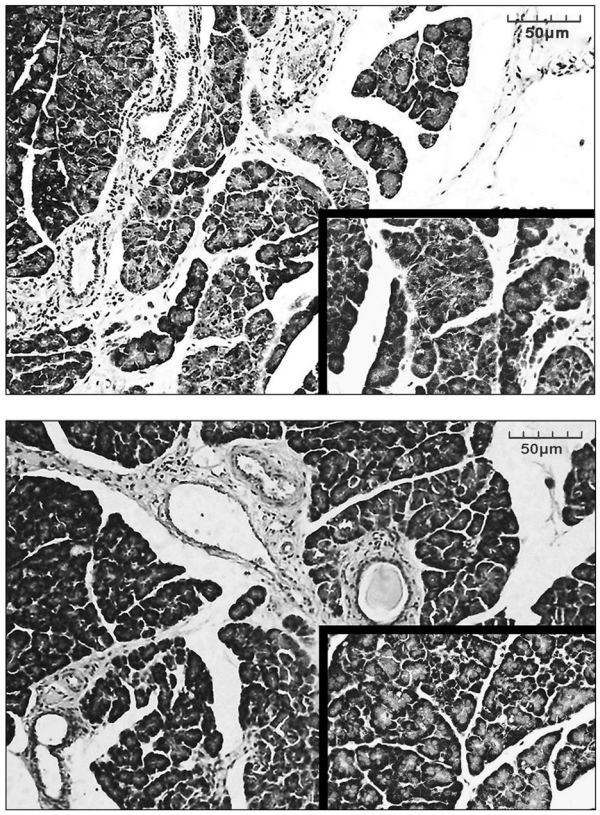

Fig. 8 Effect of the NF-κB p50 NLS on pancreatic morphological damage in CCK-induced pancreatitis. **a** A representative pancreatic sample from the Group CCK (animals treated with 2 × 100 µg/kg of CCK IP) showing marked edema, inflammatory activity, microfocal necrosis (HE × 100); and microfocal necrosis, vacuolar degeneration in the acinar cells (insert: HE × 250). Scale bar = 50 µm. **b** A representative pancreatic sample from animals receiving p50 NLS pretreatment before CCK (i.e., Group NLS + CCK): milder edema, milder acinar degeneration, and vacuolization (HE × 100 and HE × 250). Scale bar = 50 µm

Table 1 Effects of the NLS on the histologic parameters in CCK-induced acute pancreatitis

	Controls	Group CCK	Group NLS + CCK
Edema	0.1 ± 0.067**	0.9 ± 0.067	0.65 ± 0.076*
Vascular change	0.1 ± 0.067**	0.7 ± 0.082	0.45 ± 0.05*
Inflammation	0**	0.6 ± 0.07	0.35 ± 0.076*
Acinar necrosis	0**	0.75 ± 0.083	0.45 ± 0.09*
Calcification	0	0.125 ± 0,065	0
Fat necrosis	0*	0.167 ± 0.071	0.05 ± 0.05

Means + SEM of 10 animals in each group are shown

*$p < 0.05$ vs Group CCK; **$p < 0.01$ vs Group CCK

also abolished peptide uptake, highlighting the paramount role of electrostatic interactions in peptide uptake. Both ATP-depletion or low temperature blocked peptide entry, further providing evidence on the energy-dependent and temperature-sensitivite endocytic uptake mediated by polyanions of the cholesterol-enriched lipid rafts.

Proteoglycans comprise a heterogeneous group of proteins substituted with linear polysulfated and, thereby, highly negatively charged glycosaminoglycan polysaccharides (e.g. heparan sulfate) (Iozzo 2001; Letoha et al. 2006; Sarrazin et al. 2011). Cell surface proteoglycans bind a multitude of ligands and influence cellular physiology and pathology, including cytokine-signaling and inflammation (Letoha et al. 2006; Billings and Pacifici 2015; O'Callaghan et al. 2018; El Masri et al. 2020). Among cell surface proteoglycans, the SDC family of transmembrane HSPGs act as molecular ferries by attaching cationic proteins and delivering them intracellularly (Letoha et al. 2010, 2019, 2021a, 2021b, 2022; Christianson and Belting 2014; Hudak et al. 2019). SDC-mediated endocytosis occurs independently of clathrin and caveolin but in a lipid raft-dependent manner: ligands induce clustering and redistribution of SDCs to lipid rafts and stimulate the lipid raft-dependent endocytosis of the SDC-ligand complex (Payne et al. 2007; Szilak et al. 2013; Christianson and Belting 2014; Hudak et al. 2019). Besides their endocytic activity, SDCs are also heavily involved in cell signaling and transmit signals from the cell exterior to the cytoplasm (Tkachenko et al. 2005; Couchman et al. 2015; Afratis et al. 2017). Thus, the SDC-mediated uptake of the p50 NLS peptide can explain its efficient internalization and the maintenance of its ability to inhibit NF-κB-driven inflammatory pathways, as demonstrated by the inhibition of NF-κB activities in vitro and in vivo. Among SDCs, the p50 NLS peptide showed the highest affinity towards SDC4, the ubiquitously expressed member of the SDC4 family (Letoha et al. 2010, 2019; Keller-Pinter et al. 2021). Still, the overexpression of the other SDC isoforms also increased the cellular uptake of the peptide markedly. SDCs enables the entry of the peptide into a wide array of SDC-expressing cells, including, but not limited to macrophages and pancreatic acinar cells, two key cells types whose $Ca2+$ overload initiates acute pancreatitis (Uhlen et al. 2015; Gryshchenko et al. 2021; Petersen et al. 2021). During acute pancreatitis, excessive $Ca2+$ signal generation also occurs in pancreatic stellate cells, a cell type with pronounced SDC4 expression (Chronopoulos et al. 2020; Petersen et al. 2021).

In live rats, the peptide rapidly entered the pancreas, an organ exhibiting pronounced SDC expression (Uhlen et al. 2015). The observed rapidity of the peptide's in vivo internalization is also advantageous in the experimental model of CCK-induced acute pancreatitis, where NF-κB activation and nuclear translocation peak 30 min after CCK stimulation (Gukovsky et al. 1998; Letoha et al. 2006). The p50 NLS' reported broad inhibitory spectrum on the nuclear import NF-κB proteins (i.e., intracellularly delivered p50 NLS is not specific for p50, but it also blocks the nuclear import of p65 and other SRTFs) also offers significant therapeutic benefits in an acute inflammatory disorder regulated by complex NF-κB activation pathways (Torgerson et al. 1998; Boothby 2001; Wu et al. 2020). The performed EMSA showed that p50 NLS pretreatment could suppress CCK-induced nuclear translocation and DNA-binding activity of NF-κB. NF-κB inhibitory activity of the NLS peptide resulted in improved parameters of pancreatitis. Thus, pretreatment with the NF-κB p50 NLS peptide ameliorated CCK-induced cellular damage, edema and neutrophil sequestration both within the pancreas and lung. Moreover, pretreatment with the p50 NLS decreased proinflammatory cytokines and ROS production in the pancreas. Histopathological evaluation of pancreas samples also confirmed improvements due to p50 NLS treatment. Thus, the cationic NLS peptide could also preserve its NF-κB-inhibitory and anti-inflammatory effects in vivo.

In summary, our study demonstrates the efficient intracellular delivery of a cationic NLS peptide to inhibit NF-κB-dependent inflammatory pathways and provides preclinical proof of concept on the efficient utilization of SDC-mediated peptide transduction to modulate acute inflammation of the pancreas.

Materials and Methods

Peptide Synthesis and Labeling

The NF-κB p50 NLS peptide (CYVQRKRQKLMP) and its Gly analog (GlyNLS, CYVQGGGQGLMP) were synthesized in solid phase by standard methodology as described previously (Torgerson et al. 1998). For the uptake experiments, the peptides were labeled with fluorescein isothiocyanate (FITC; cat. no. 46950; Sigma-Aldrich, Darmstadt, Germany) as described by Fulop et al. (2001). CCK was prepared with the method of Penke et al. (1984).

Cell Lines

Human microvascular endothelial HMEC-1 cells (ATCC, Manassas, VA, USA, cat. no. CRL-3243), murine L929 fibroblasts (Merck KGaA, Darmstadt, Germany; cat. no. 85011425-1VL) and RAW 264.7 macrophages (ATCC, cat. no. TIB-71) were cultured as described previously (Letoha et al. 2005a, b, c, 2006). AR42J rat pancreatic acinar cells (ATCC, cat. no. 30-2004) were cultured in F12 medium (with 20% FBS) according to the guidelines of ATCC. Full-length SDC1-4 transfectants, established in K562 cells (ATCC, cat. no. CCL-243), were created as described

previously (Supplementary Fig. S3) (Letoha et al. 2019; Hudák et al. 2021). Stable SDC transfectants were selected by measuring SDC expression with flow cytometry using APC-labeled SDC antibodies specific for the respective SDC isoform as described previously (Letoha et al. 2019; Hudak et al. 2021b). HS expression of the applied SDC transfectants were measured with flow cytometry by using anti-human HS antibody (10E4 epitope; cat.no. 370255-S; Amsbio, Abingdon, UK) with Alexa Fluor (AF) 647-labeled secondary anti-mouse IgM and respective isotype control (cat. no. 02-6800; Thermo Fisher Scientific, Waltham, MA, USA), as described previously(Letoha et al. 2019; Hudak et al. 2021b).

Cell Viability Measurements

The effect of the applied peptides (NLS and its GlyNLS analog) on cell viability was assessed with the EZ4U cell proliferation assay (Biomedica Gmbh, Vienna, Austria, cat. no. BI-5000), according to the instructions of the manufacturer (Hudak et al. 2021b). Absorbance was measured with a BioTek Cytation 3 multimode microplate reader.

Confocal Laser Scanning Microscopy

Internalization of the FITC-labeled p50 NLS peptide into L929, RAW 264.7 and HMEC-1 cells was visualized by confocal laser scanning microscopy. Cells were preincubated in Opti-MEM (cat. no. 31985062; Thermo Fisher Scientific, Waltham, MA, USA) at either 37 or 4 °C for 30 min before incubation with the peptides(Letoha et al. 2006). The peptide solution was prepared at a concentration of 20 µM in Opti-MEM by diluting a 1 mM stock solution of peptide in phosphate-buffered saline (PBS) (Letoha et al. 2005a, b, c). After various amounts of time (30, 60, 90 min) at 37 and 0 °C, the cells were rinsed three times with ice-cold PBS, and fluorescence distribution was immediately analyzed on an Olympus FV1000 confocal laser scanning microscope. Excitation was obtained with an Argon ion laser set at 488 nm for FITC excitation and the emitted light was filtered with an appropriate long-pass filter (514 nm). Sections presented were taken approximately at the mid-height level of the cells. Photomultiplier gain and laser power were identical within each experiment. Cell viability was routinely determined by using trypan blue exclusion tests (Letoha et al. 2005a, b, c).

Flow Cytometry Analysis of Peptide Uptake

L929 fibroblasts, RAW 264.7 macrophages, and HMEC-1 cells were used to quantify the cellular internalization of the fluorescent peptide. 6×10^5 cells/mL in Opti-MEM were incubated with the FITC-labeled peptide (at a concentration of 20 µM) at 37 and 4 °C for 30, 60 and 90 min, respectively. The cells were washed twice and resuspended in 0.5 mL of physiological saline. Equal volumes of this suspension and a stock solution of trypan blue (cat. no: T6146-5G; Merck KGaA, Darmstadt, Germany; 500 µg/mL dissolved in ice-cold 0.1 M citrate buffer at pH 4.0) were allowed to mix for 1 min before FACS analyses. In this way, sample pH was lowered to pH 4.0, thereby optimizing the quenching effect of trypan blue (Sahlin et al. 1983). Cellular uptake was measured with flow cytometry using a FACScan (Becton Dickinson, Franlin Lakes, NJ, USA). A minimum of 10,000 events per sample was analyzed. The viability of the cells was determined by appropriate gating in a forward-scatter-against-side-scatter plot to exclude dead cells, debris, and aggregates (Letoha et al. 2005a, b, c).

To investigate the involvement of cholesterol-rich membrane domains (lipid rafts) in peptide uptake, cells were pretreated with 5 mM methyl-β-cyclodextrin (MCD; Sigma-Aldrich, cat.no: C4555-5G) for 60 min at 37 °C and then treated as mentioned above(Letoha et al. 2005a, b, c). To study the role of polyanionic cell-surface proteoglycans the cells were incubated with the FITC-labeled peptides in the presence of HS (25 µg/mL; Sigma-Aldrich; cat. no. H4777-1MG) in Opti-MEM and then processed as usual for the FACS analyses.

To block endocytosis, cells were either incubated at 4 °C or their cellular ATP pools were depleted. For experiments at 4 °C, the cells were maintained for 30 min on ice before peptide incubation and throughout the experiments (Letoha et al. 2005a, b, c). To induce ATP depletion, the cells were incubated with 0.1% sodium azide (Sigma-Aldrich; cat.no. S2002-5G) and 50 mM 2-deoxy-D-glucose (Sigma-Aldrich; cat.no. D8375-1G) in Opti-MEM for 60 min before the addition of peptides at 37 °C (Fischer et al. 2004).

Imaging Flow Cytometry Analysis of Peptide Uptake

WT K562, SDC transfectants or AR42J cells were utilized to quantify the internalization of the FITC-labeled p50 NLS peptide. Briefly, 6×10^5 cells/mL in DMEM/F12 medium were incubated with FITC-labeled p50 NLS or its Gly analog (at a concentration of 20 µM) for 90 min (15 min for AR42J) at 37 °C (Letoha et al. 2005a, b, c). After incubation with the, the cells were trypsinized (with the method described by Nakase et al.) to remove the extracellularly attached peptides from the cell surface (Nakase et al. 2007; Hudak et al. 2019, 2021b, 2022). The cells were then rinsed three times with PBS containing 1% BSA and progressed towards flow cytometry. Cellular uptake was then measured with flow cytometry using an Amnis FlowSight imaging flow cytometer (Amnis Corporation, Seattle, WA, USA). A minimum of 10,000 events per sample was analyzed. Appropriate gating in a forward-scatter-against-side-scatter plot was utilized to exclude cellular debris and aggregates.

Fluorescence analysis was conducted with the Amnis IDEAS analysis software (Hudak et al. 2021b).

Transformation of Cell Lines

Mouse L929 cells (5×10^5/60 mm plate) were transformed with pNF-κB-luc4 and pSV-2/neo plasmids (coding for firefly luciferase under the control of 5 NF-κB-responsive elements and the neo^r gene controlled by the SV40 enhancer/promoter, respectively) using the DMRIE-C cationic lipid transfection agent (Thermo Fisher Scientific; cat. no. 10459014) as described previously (Letoha et al. 2005a, b, c). Selection started 48 h later; the cells were exposed to geneticin (400 mg/L; Sigma-Aldrich) for two weeks, refreshing the medium twice weekly. Clones were isolated and tested for the intensity of their TNF-α-elicited NF-κB induction (50–100 U/mL recombinant TNF-α, 6–10 h of induction time). RAW 264.7 cells (5×10^5/60 mm plate) subcultured the previous day were transformed overnight with the above plasmids complexed with polyethylene-imine (jetPEI, cat. no. 101000053; Vectura, Illkirch, France) as described previously (Letoha et al. 2005a, b, c).

Luciferase Assays

Luciferase assays on 1 day-old cultures of L929 and RAW 264.7 cells transformed with pNF-κB-luc4 and pSV-2/neo plasmids were carried out as described previously (Letoha et al. 2005a, b, c, 2006). Briefly, 3×10^4 cells/well (in MIX MEM 10% FCS) were exposed to various concentrations (0.39 to 25 uM) of the p50 NLS peptide for 30 min. Then the cells were treated with TNF-α (10 U/mL) or LPS (30 ng/mL) in 100 µL of the above medium per well (Letoha et al. 2005a, b, c, 2006). After 6 h of incubation with TNF-α or LPS, the medium was removed and the cells were washed and lysed for 10 min at room temperature in Reporter Lysis Buffer (20 µL/well; cat. no. E4030; Promega Co., Madison, WI, USA) (Letoha et al. 2005a, b, c, 2006). The substrate was added (20 µL/well; Promega Co.) and luciferase activity was measured in a BioTek Cytation 3 Cell Imaging Multi-Mode Plate Reader (BioTek, Winooski, VT, USA). Control cells received TNF-α (10 U/mL) or LPS (30 ng/mL) treatment only and processed as mentioned above. Cell viability was assessed by trypan blue exclusion assays (Letoha et al. 2005a, b, c, 2006).

ICAM-1 Expression

ICAM-1 expression of HMEC-1 cells, grown on microplates (Corning Life Sciences), was conducted as described previously (Letoha et al. 2005a, b, c, 2006). 3×10^4 cells/well in HE-SFM 2% FCS were exposed to various concentrations (3.13 to 50 uM) of the p50 NLS peptide for 30 min. Thirty minutes later the cells were treated with TNF-α (10 U/mL in 100 µL of the above medium per well). After 6 h of incubation with TNF-α, the cells were trypsinized, washed and resuspended in 10% FCS, then vortexed for 5 min at 2000 rpm, resuspended in PBS and vortexed again for 5 min. Then the medium was removed and the cells were incubated in PBS with the FITC-conjugated monoclonal mouse anti-human ICAM-1 antibody (5–10 µg/mL; cat. no. BMS108FI; Thermo Fischer Scientific) for 30 min on ice. After two washes and fixation with 2% paraformaldehyde, while being vortexed, the samples were analyzed by flow cytometry using the FACScan flow cytometer and the CellQuest analysis program (Becton Dickinson). Control cells received only TNF-α treatment (Letoha et al. 2006). The viability of the cells was determined by concurrent propidium iodide (10 µg/mL; Sigma-Aldrich; cat. no. P4170-250MG) staining and appropriate gating in a forward-scatter-against-side-scatter plot to exclude dead cells, debris, and aggregates (Letoha et al. 2005a, b, c).

In Vivo Uptake Experiments

In vivo uptake studies in male Wistar rats (provided by the Animal Center of the Biological Research Center) weighing 250–300 g were carried out as described previously (Letoha et al. 2005a, b, c, 2006, 2007). The animals were kept at a constant room temperature with a 12 h light–dark cycle and were allowed free access to water and standard laboratory chow (Innovo Kft., Isaszeg, Hungary). All animal experiments were performed according to national and institutional ethical guidelines. The animal study protocol was approved by the Institutional Animal Ethics Committee of the Biological Research Centre and by the National Scientific Ethical Committee on Animal Experimentation (protocol code XVI./04714/001/2006., approved on 08 March 2006) and complied with the European Communities Council Directive of 24 November 1986 (86/609/EEC). Six animals were intraperitoneally (IP) injected with 20 nM/kg of the FITC-labeled p50 NLS peptide (in 0.5 mL PBS). Control animals (n = 6) received IP injections of 0.5 mL PBS. Rats were anesthetized (with pentobarbital sodium 50 mg/kg IP) and killed 15 min after the injections by exsanguinations through the abdominal aorta. Pancreas tissues were harvested and frozen in HistoPrep media (cat. no. SH75-125D; Thermo Fisher Scientific). Sections (10 to 50 µm) were cut on a cryostat and analyzed with fluorescence microscopy (BioTek Cytation 3). The fluorescence signals detected were measured with BioTek Gen5 Software. The animal study is reported in accordance with ARRIVE guidelines (Animal Research: Reporting of In Vivo Experiments).

CCK-Induced Pancreatitis

CCK-induced pancreatitis utilizing various experimental groups of rats (each group contained 10 animals) was carried out as described previously (Letoha et al. 2005a, b, c, 2006, 2007). The rats were fasted for 16 h then acute pancreatitis was induced by injecting 100 µg/kg body weight of CCK (dissolved in PBS) IP twice at an interval of 1 h ("Group CCK"). The p50 NLS pretreated group ("Group NLS + CCK") received 2 mg/kg body weight of the NF-κB p50 NLS peptide (in PBS) IP 30 min before the first injection of CCK. Control rats received 3 × 0.5 mL PBS IP instead of CCK or the NF-κB p50 NLS. Anesthetized (pentobarbital sodium; 50 mg/kg IP; Sigma Aldrich; cat. no. P3761) rats were killed by exsanguinations through the abdominal aorta 4 h after the first CCK injection (Letoha et al. 2005a, b, c, 2006, 2007). The pancreas and lungs were quickly removed, cleaned of fat and lymph nodes, weighed, frozen in liquid nitrogen and stored at − 80 °C until use (Letoha et al. 2005a, b, c, 2006, 2007).

Electrophoretic Mobility Shift Assay (EMSA) of NF-κB

The EMSA was carried out as described previously (Letoha et al. 2005a, b, c, 2006).

Western Blotting

Western blot analysis of pancreatic IκB-α was performed as described previously (Letoha et al. 2006). β-tubulin (mouse monoclonal, Santa Cruz Biotechnology (Dallas, TX, USA), Inc., cat. no. sc-5274) was used as loading control (Hudak et al. 2021b).

Molecular Markers of Acute Pancreatitis

Molecular markers of acute pancreatitis were analyzed as described previously (Letoha et al. 2005a, b, c, 2006, 2007). The pancreatic weight/body weight ratio was utilized to evaluate the degree of pancreatic edema. The serum levels of amylase were determined by a colorimetric kinetic method (cat. no. D96569; Dialab, Vienna, Austria). All blood samples were centrifuged at 2500×*g* for 20 min. Tumor necrosis factor-α (TNF-α) and IL-6 concentrations were measured in the pancreatic cytosolic fractions with ELISA kits (cat. no. ERA57RB and ERA32RB; all Thermo Fisher Scientific) according to the manufacturers' instructions. As a marker of tissue leukocyte infiltration, pancreatic and lung MPO activity was assessed by Kuebler et al. (Kuebler et al. 1996). Pancreatic MDA level was measured after the reaction with thiobarbituric acid, according to the method of Placer et al., and was also corrected for the protein content of the tissue (Placer et al. 1966). GSH level was determined spectrophotometrically with Ellman's reagent (Sedlak and Lindsay 1968).

Histological Evaluation of CCK-Induced Acute Pancreatitis

Histological evaluation of CCK-induced acute pancreatitis was carried out as described previously (Letoha et al. 2005a, b, c, 2006, 2007). A portion of the pancreas was fixed in 8% neutral formaldehyde solution (Sigma-Aldrich; cat. no. 47608) and subsequently embedded in paraffin (Sigma-Aldrich; cat. no. P3558). Sections were cut at 4 µm thickness and stained with hematoxylin and eosin (cat. no. ab245880; Abcam, Waltham, MA, USA). The slides were coded and read for the traditional histological markers of pancreatic tissue injury by two independent observers who were blind to the experimental protocol. They used the scoring system of Hughes et al. for the evaluation of acute pancreatitis (Hughes et al. 1996). Thus, semiquantitative grading of interstitial edema (0–1), vascular changes (0–2), inflammation (0–1), acinar necrosis (0–2) calcification (0–0.5) and fat necrosis (0–0.5) of the pancreas samples was evaluated in each animal (described in more details in Table 2).

Statistical Analysis

Results are expressed as means + standard error of the mean (SEM). Differences between experimental groups were evaluated by using one-way analysis of variance (ANOVA). Values of $p < 0.05$ were accepted as significant (Hudak et al. 2019; Letoha et al. 2019).

Supplementary Information The online version contains supplementary material available at https://doi.org/10.1007/s10989-023-10548-9.

Author Contributions AL, AH, ZB, LS, CV, and TL performed the experimental work and analyzed the data. ZB synthesized the peptides. AH and TL performed the microscopy studies. LS constructed the SDC plasmids. TL, LA conceived the project, analyzed data, and drafted the manuscript. TL supervised and coordinated the project. All authors have approved the final article.

Funding A.H., G.V., L.S. and T.L. received funding from the Innovative Medicines Initiative 2 Joint Undertaking, under grant agreement No 807015. This Joint Undertaking receives support from the European Union's Horizon 2020 research and innovation program and EFPIA. A.H., L.S., and T.L. were also supported by the grants 2017-2.3.6-TÉT-CN-2018-00023 and 2019-2.1.1-EUREKA-2019-00007. A.H., T.L., A.L., C.V. and L.S. were also supported by the grants 2020-1.1.6-JÖVŐ-2021-00012 and 2020-1.1.2-PIACI-KFI-2021-00233 of the National Research, Development, and Innovation Office, Hungary.

Data Availability All data and materials are available in the manuscript, the supplementary information, or from the corresponding authors upon reasonable request.

Table 2 Histological scoring system for the evaluation of pancreatitis

	0	0.5	1	1.5	2
Edema	Absent	Focal < 50%	Diffuse > 50%		
Vascular change	Absent	Congestion	focal Haemorrhage	Diffuse haemorrhage	Vascular necrosis or thrombosis
Inflammation	Absent	Focal/mild	Diffuse > 50%		
Acinar necrosis	Absent	Single acinar cell Necrosis/ foci of peripheral lobular damage	Lobular necrosis in 10% to 30% of the surface area	Lobular necrosis in 30% to 50% of the surface area	Lobular necrosis in > 50% of the surface area/microabscesses
Calcificatin	Absent	Present			
Fat necrosis	Absent	Present			

Declarations

Conflicts of interest The authors declare no conflicts of interest.

References

Afratis NA, Nikitovic D, Multhaupt HA, Theocharis AD, Couchman JR, Karamanos NK (2017) Syndecans key regulators of cell signaling and biological functions. FEBS J 284:27–41

Ahmed M (2017) Peptides, polypeptides and peptide-polymer hybrids as nucleic acid carriers. Biomater Sci 5:2188–2211

Akuta T, Eguchi A, Okuyama H, Senda T, Inokuchi H, Suzuki Y, Nagoshi E, Mizuguchi H, Hayakawa T, Takeda K, Hasegawa M, Nakanishi M (2002) Enhancement of phage-mediated gene transfer by nuclear localization signal. Biochem Biophys Res Commun 297:779–786

Arenal A, Pimentel R, Garcia C, Pimentel E, Alestrom P (2004) The SV40 T antigen nuclear localization sequence enhances nuclear import of vector DNA in embryos of a crustacean (*Litopenaeus schmitti*). Gene 337:71–77

Bathori G, Cervenak L, Karadi I (2004) Caveolae–an alternative endocytotic pathway for targeted drug delivery. Crit Rev Ther Drug Carrier Syst 21:67–95

Belting M (2003) Heparan sulfate proteoglycan as a plasma membrane carrier. Trends Biochem Sci 28:145–151

Billings PC, Pacifici M (2015) Interactions of signaling proteins, growth factors and other proteins with heparan sulfate: mechanisms and mysteries. Connect Tissue Res 56:272–280

Bohmova E, Machova D, Pechar M, Pola R, Venclikova K, Janouskova O, Etrych T (2018) Cell-penetrating peptides: a useful tool for the delivery of various cargoes into cells. Physiol Res 67:S267–S279

Boothby M (2001) Specificity of sn50 for NF-kappa B? Nat Immunol 2:471–472

Cagno V, Tseligka ED, Jones ST, Tapparel C (2019) Heparan sulfate proteoglycans and viral attachment: true receptors or adaptation bias? Viruses 11:596

Christianson HC, Belting M (2014) Heparan sulfate proteoglycan as a cell-surface endocytosis receptor. Matrix Biol 35:51–55

Chronopoulos A, Thorpe SD, Cortes E, Lachowski D, Rice AJ, Mykuliak VV, Rog T, Lee DA, Hytonen VP, Del Rio Hernandez AE (2020) Syndecan-4 tunes cell mechanics by activating the kindlin-integrin-RhoA pathway. Nat Mater 19:669–678

Console S, Marty C, Garcia-Echeverria C, Schwendener R, Ballmer-Hofer K (2003) Antennapedia and HIV transactivator of transcription (TAT) "protein transduction domains" promote endocytosis of high molecular weight cargo upon binding to cell surface glycosaminoglycans. J Biol Chem 278:35109–35114

Couchman JR, Gopal S, Lim HC, Norgaard S, Multhaupt HA (2015) Fell-Muir lecture: syndecans: from peripheral coreceptors to mainstream regulators of cell behaviour. Int J Exp Pathol 96:1–10

De Pasquale V, Quiccione MS, Tafuri S, Avallone L, Pavone LM (2021) Heparan sulfate proteoglycans in viral infection and treatment: a special focus on SARS-CoV-2. Int J Mol Sci 22:10

Derossi D, Joliot AH, Chassaing G, Prochiantz A (1994) The third helix of the Antennapedia homeodomain translocates through biological membranes. J Biol Chem 269:10444–10450

Derossi D, Calvet S, Trembleau A, Brunissen A, Chassaing G, Prochiantz A (1996) Cell internalization of the third helix of the Antennapedia homeodomain is receptor-independent. J Biol Chem 271:18188–18193

Derossi D, Chassaing G, Prochiantz A (1998) Trojan peptides: the penetratin system for intracellular delivery. Trends Cell Biol 8:84–87

Dougherty PG, Sahni A, Pei D (2019) Understanding cell penetration of cyclic peptides. Chem Rev 119:10241–10287

Drin G, Cottin S, Blanc E, Rees AR, Temsamani J (2003) Studies on the internalization mechanism of cationic cell-penetrating peptides. J Biol Chem 278:31192–31201

Eguchi A, Akuta T, Okuyama H, Senda T, Yokoi H, Inokuchi H, Fujita S, Hayakawa T, Takeda K, Hasegawa M, Nakanishi M (2001) Protein transduction domain of HIV-1 Tat protein promotes efficient delivery of DNA into mammalian cells. J Biol Chem 276:26204–26210

El Masri R, Cretinon Y, Gout E, Vives RR (2020) HS and inflammation: a potential playground for the sulfs? Front Immunol 11:570

Elfenbein A, Simons M (2013) Syndecan-4 signaling at a glance. J Cell Sci 126:3799–3804

Favretto ME, Wallbrecher R, Schmidt S, van de Putte R, Brock R (2014) Glycosaminoglycans in the cellular uptake of drug delivery vectors—bystanders or active players? J Control Release 180:81–90

Fischer R, Kohler K, Fotin-Mleczek M, Brock R (2004) A stepwise dissection of the intracellular fate of cationic cell-penetrating peptides. J Biol Chem 279:12625–12635

Fittipaldi A, Ferrari A, Zoppe M, Arcangeli C, Pellegrini V, Beltram F, Giacca M (2003) Cell membrane lipid rafts mediate caveolar endocytosis of HIV-1 Tat fusion proteins. J Biol Chem 278:34141–34149

Fulop L, Penke B, Zarandi M (2001) Synthesis and fluorescent labeling of beta-amyloid peptides. J Pept Sci 7:397–401

Futaki S, Nakase I, Tadokoro A, Takeuchi T, Jones AT (2007) Arginine-rich peptides and their internalization mechanisms. Biochem Soc Trans 35:784–787

Gallay P (2004) Syndecans and HIV-1 pathogenesis. Microbes Infect 6:617–622

Gryshchenko O, Gerasimenko JV, Petersen OH, Gerasimenko OV (2021) Calcium signaling in pancreatic immune cells in situ. Function (oxf) 2:zqaa026

Gukovsky I, Gukovskaya A (2013) Nuclear factor-kappaB in pancreatitis: jack-of-all-trades, but which one is more important? Gastroenterology 144:26–29

Gukovsky I, Gukovskaya AS, Blinman TA, Zaninovic V, Pandol SJ (1998) Early NF-kappaB activation is associated with hormone-induced pancreatitis. Am J Physiol 275:G1402–G1414

Gukovsky I, Reyes CN, Vaquero EC, Gukovskaya AS, Pandol SJ (2003) Curcumin ameliorates ethanol and nonethanol experimental pancreatitis. Am J Physiol Gastrointest Liver Physiol 284:G85-95

Heitz F, Morris MC, Divita G (2009) Twenty years of cell-penetrating peptides: from molecular mechanisms to therapeutics. Br J Pharmacol 157:195–206

Huang H, Liu Y, Daniluk J, Gaiser S, Chu J, Wang H, Li ZS, Logsdon CD, Ji B (2013) Activation of nuclear factor-kappaB in acinar cells increases the severity of pancreatitis in mice. Gastroenterology 144:202–210

Hudak A, Kusz E, Domonkos I, Josvay K, Kodamullil AT, Szilak L, Hofmann-Apitius M, Letoha T (2019) Contribution of syndecans to cellular uptake and fibrillation of alpha-synuclein and tau. Sci Rep 9:16543

Hudak A, Josvay K, Domonkos I, Letoha A, Szilak L, Letoha T (2021a) The interplay of apoes with syndecans in influencing key cellular events of amyloid pathology. Int J Mol Sci 22:7070

Hudak A, Letoha A, Szilak L, Letoha T (2021b) Contribution of syndecans to the cellular entry of SARS-CoV-2. Int J Mol Sci 22:5336

Hudak A, Veres G, Letoha A, Szilak L, Letoha T (2022) Syndecan-4 is a key facilitator of the SARS-CoV-2 delta variant's superior transmission. Int J Mol Sci 23:796

Hughes CB, Grewal HP, Gaber LW, Kotb M, El-din ABM, Mann L, Osama Gaber A (1996) Anti-TNFα therapy improves survival and ameliorates the pathophysiologic sequelae in acute pancreatitis in the rat. Am J Surg 171:274–280

Iozzo RV (2001) Heparan sulfate proteoglycans: intricate molecules with intriguing functions. J Clin Invest 108:165–167

Keller-Pinter A, Gyulai-Nagy S, Becsky D, Dux L, Rovo L (2021) Syndecan-4 in tumor cell motility. Cancers (basel) 13:3322

Kirkham M, Parton RG (2005) Clathrin-independent endocytosis: new insights into caveolae and non-caveolar lipid raft carriers. Biochim Biophys Acta 1746:349–363

Kiss AL, Botos E (2009) Endocytosis via caveolae: alternative pathway with distinct cellular compartments to avoid lysosomal degradation? J Cell Mol Med 13:1228–1237

Kolenko V, Bloom T, Rayman P, Bukowski R, Hsi E, Finke J (1999) Inhibition of NF-kappa B activity in human T lymphocytes induces caspase-dependent apoptosis without detectable activation of caspase-1 and -3. J Immunol 163:590–598

Kuebler WM, Abels C, Schuerer L, Goetz AE (1996) Measurement of neutrophil content in brain and lung tissue by a modified myeloperoxidase assay. Int J Microcirc Clin Exp 16:89–97

Kumari S, Mg S, Mayor S (2010) Endocytosis unplugged: multiple ways to enter the cell. Cell Res 20:256–275

LeCher JC, Nowak SJ, McMurry JL (2017) Breaking in and busting out: cell-penetrating peptides and the endosomal escape problem. Biomol Concepts 8:131–141

Letoha T, Gaal S, Somlai C, Czajlik A, Perczel A, Penke B (2003) Membrane translocation of penetratin and its derivatives in different cell lines. J Mol Recognit 16:272–279

Letoha T, Gaal S, Somlai C, Venkei Z, Glavinas H, Kusz E, Duda E, Czajlik A, Petak F, Penke B (2005a) Investigation of penetratin peptides. Part 2. In vitro uptake of penetratin and two of its derivatives. J Pept Sci 11:805–811

Letoha T, Somlai C, Takacs T, Szabolcs A, Jarmay K, Rakonczay Z Jr, Hegyi P, Varga I, Kaszaki J, Krizbai I, Boros I, Duda E, Kusz E, Penke B (2005b) A nuclear import inhibitory peptide ameliorates the severity of cholecystokinin-induced acute pancreatitis. World J Gastroenterol 11:990–999

Letoha T, Somlai C, Takacs T, Szabolcs A, Rakonczay Z Jr, Jarmay K, Szalontai T, Varga I, Kaszaki J, Boros I, Duda E, Hackler L, Kurucz I, Penke B (2005c) The proteasome inhibitor MG132 protects against acute pancreatitis. Free Radic Biol Med 39:1142–1151

Letoha T, Kusz E, Papai G, Szabolcs A, Kaszaki J, Varga I, Takacs T, Penke B, Duda E (2006) In vitro and in vivo nuclear factor-kappaB inhibitory effects of the cell-penetrating penetratin peptide. Mol Pharmacol 69:2027–2036

Letoha T, Feher LZ, Pecze L, Somlai C, Varga I, Kaszaki J, Toth G, Vizler C, Tiszlavicz L, Takacs T (2007) Therapeutic proteasome inhibition in experimental acute pancreatitis. World J Gastroenterol 13:4452–4457

Letoha T, Keller-Pinter A, Kusz E, Kolozsi C, Bozso Z, Toth G, Vizler C, Olah Z, Szilak L (2010) Cell-penetrating peptide exploited syndecans. Biochim Biophys Acta 1798:2258–2265

Letoha T, Hudak A, Kusz E, Pettko-Szandtner A, Domonkos I, Josvay K, Hofmann-Apitius M, Szilak L (2019) Contribution of syndecans to cellular internalization and fibrillation of amyloid-beta(1–42). Sci Rep 9:1393

Lin YZ, Yao SY, Veach RA, Torgerson TR, Hawiger J (1995) Inhibition of nuclear translocation of transcription factor NF-kappa B by a synthetic peptide containing a cell membrane-permeable motif and nuclear localization sequence. J Biol Chem 270:14255–14258

Liu XY, Robinson D, Veach RA, Liu D, Timmons S, Collins RD, Hawiger J (2000) Peptide-directed suppression of a pro-inflammatory cytokine response. J Biol Chem 275:16774–16778

Liu M, Fang X, Yang Y, Wang C (2021) Peptide-enabled targeted delivery systems for therapeutic applications. Front Bioeng Biotechnol 9:701504

Montrose K, Yang Y, Sun X, Wiles S, Krissansen GW (2013) Xentry, a new class of cell-penetrating peptide uniquely equipped for delivery of drugs. Sci Rep 3:1661

Nakanishi M, Eguchi A, Akuta T, Nagoshi E, Fujita S, Okabe J, Senda T, Hasegawa M (2003) Basic peptides as functional components of non-viral gene transfer vehicles. Curr Protein Pept Sci 4:141–150

Nakase I, Tadokoro A, Kawabata N, Takeuchi T, Katoh H, Hiramoto K, Negishi M, Nomizu M, Sugiura Y, Futaki S (2007) Interaction of arginine-rich peptides with membrane-associated proteoglycans is crucial for induction of actin organization and macropinocytosis. Biochemistry 46:492–501

Nichols B (2003) Caveosomes and endocytosis of lipid rafts. J Cell Sci 116:4707–4714

Nichols BJ, Lippincott-Schwartz J (2001) Endocytosis without clathrin coats. Trends Cell Biol 11:406–412

O'Callaghan P, Zhang X, Li JP (2018) Heparan sulfate proteoglycans as relays of neuroinflammation. J Histochem Cytochem 66:305–319

Oehlke J, Beyermann M, Wiesner B, Melzig M, Berger H, Krause E, Bienert M (1997) Evidence for extensive and non-specific translocation of oligopeptides across plasma membranes of mammalian cells. Biochim Biophys Acta 1330:50–60

Parolini I, Sargiacomo M, Galbiati F, Rizzo G, Grignani F, Engelman JA, Okamoto T, Ikezu T, Scherer PE, Mora R, Rodriguez-Boulan E, Peschle C, Lisanti MP (1999) Expression of caveolin-1 is required for the transport of caveolin-2 to the plasma membrane. Retention of caveolin-2 at the level of the golgi complex. J Biol Chem 274:25718–25725

Parton RG, Richards AA (2003) Lipid rafts and caveolae as portals for endocytosis: new insights and common mechanisms. Traffic 4:724–738

Payne CK, Jones SA, Chen C, Zhuang X (2007) Internalization and trafficking of cell surface proteoglycans and proteoglycan-binding ligands. Traffic 8:389–401

Penke B, Hajnal F, Lonovics J, Holzinger G, Kadar T, Telegdy G, Rivier J (1984) Synthesis of potent heptapeptide analogues of cholecystokinin. J Med Chem 27:845–849

Petersen OH, Gerasimenko JV, Gerasimenko OV, Gryshchenko O, Peng S (2021) The roles of calcium and ATP in the physiology and pathology of the exocrine pancreas. Physiol Rev 101:1691–1744

Placer ZA, Cushman LL, Johnson BC (1966) Estimation of product of lipid peroxidation (malonyl dialdehyde) in biochemical systems. Anal Biochem 16:359–364

Poon GM, Gariepy J (2007) Cell-surface proteoglycans as molecular portals for cationic peptide and polymer entry into cells. Biochem Soc Trans 35:788–793

Ragin AD, Chmielewski J (2004) Probing essential residues for cellular uptake with a cationic nuclear localization signal sequence. J Pept Res 63:155–160

Ragin AD, Morgan RA, Chmielewski J (2002) Cellular import mediated by nuclear localization signal Peptide sequences. Chem Biol 9:943–948

Richard JP, Melikov K, Vives E, Ramos C, Verbeure B, Gait MJ, Chernomordik LV, Lebleu B (2003) 'Cell-penetrating peptides. A reevaluation of the mechanism of cellular uptake. J Biol Chem 278:585–590

Sahlin S, Hed J, Rundquist I (1983) Differentiation between attached and ingested immune complexes by a fluorescence quenching cytofluorometric assay. J Immunol Methods 60:115–124

Sanchez-Navarro M (2021) Advances in peptide-mediated cytosolic delivery of proteins. Adv Drug Deliv Rev 171:187–198

Sandgren S, Cheng F, Belting M (2002) Nuclear targeting of macromolecular polyanions by an HIV-Tat derived peptide role for cell-surface proteoglycans. J Biol Chem 277:38877–38883

Sarrazin S, Lamanna WC, Esko JD (2011) Heparan sulfate proteoglycans. Cold Spring Harb Perspect Biol 3:a004952

Sedlak J, Lindsay RH (1968) Estimation of total, protein-bound, and nonprotein sulfhydryl groups in tissue with Ellman's reagent. Anal Biochem 25:192–205

Shafti-Keramat S, Handisurya A, Kriehuber E, Meneguzzi G, Slupetzky K, Kirnbauer R (2003) Different heparan sulfate proteoglycans serve as cellular receptors for human papillomaviruses. J Virol 77:13125–13135

Shoari A, Tooyserkani R, Tahmasebi M, Lowik DWPM (2021) Delivery of various cargos into cancer cells and tissues via cell-penetrating peptides: a review of the last decade. Pharmaceutics 13:1391

Snyder EL, Dowdy SF (2001) Protein/peptide transduction domains: potential to deliver large DNA molecules into cells. Curr Opin Mol Ther 3:147–152

Sousa de Almeida M, Susnik E, Drasler B, Taladriz-Blanco P, Petri-Fink A, Rothen-Rutishauser B (2021) Understanding nanoparticle endocytosis to improve targeting strategies in nanomedicine. Chem Soc Rev 50:5397–5434

Stow JL, Hung Y, Wall AA (2020) Macropinocytosis: insights from immunology and cancer. Curr Opin Cell Biol 65:131–140

Szilak L, Letoha T, Ughy B (2013) What is the potential of syndecan-4-targeted novel delivery technologies? Ther Deliv 4:1479–1481

Tarvirdipour S, Skowicki M, Schoenenberger CA, Palivan CG (2021) Peptide-assisted nucleic acid delivery systems on the rise. Int J Mol Sci 22:9092

Tkachenko E, Rhodes JM, Simons M (2005) Syndecans: new kids on the signaling block. Circ Res 96:488–500

Torgerson TR, Colosia AD, Donahue JP, Lin YZ, Hawiger J (1998) Regulation of NF-kappa B, AP-1, NFAT, and STAT1 nuclear import in T lymphocytes by noninvasive delivery of peptide carrying the nuclear localization sequence of NF-kappa B p50. J Immunol 161:6084–6092

True AL, Rahman A, Malik AB (2000) Activation of NF-kappaB induced by H(2)O(2) and TNF-alpha and its effects on ICAM-1 expression in endothelial cells. Am J Physiol Lung Cell Mol Physiol 279:L302–L311

Uhlen M, Bjorling E, Agaton C, Szigyarto CA, Amini B, Andersen E, Andersson AC, Angelidou P, Asplund A, Asplund C, Berglund L, Bergstrom K, Brumer H, Cerjan D, Ekstrom M, Elobeid A, Eriksson C, Fagerberg L, Falk R, Fall J, Forsberg M, Bjorklund MG, Gumbel K, Halimi A, Hallin I, Hamsten C, Hansson M, Hedhammar M, Hercules G, Kampf C, Larsson K, Lindskog M, Lodewyckx W, Lund J, Lundeberg J, Magnusson K, Malm E, Nilsson P, Odling J, Oksvold P, Olsson I, Oster E, Ottosson J, Paavilainen L, Persson A, Rimini R, Rockberg J, Runeson M, Sivertsson A, Skollermo A, Steen J, Stenvall M, Sterky F, Stromberg S, Sundberg M, Tegel H, Tourle S, Wahlund E, Walden A, Wan J, Wernerus H, Westberg J, Wester K, Wrethagen U, Xu LL, Hober S, Ponten F (2005) A human protein atlas for normal and cancer tissues based on antibody proteomics. Mol Cell Proteomics 4:1920–1932

Uhlen M, Fagerberg L, Hallstrom BM, Lindskog C, Oksvold P, Mardinoglu A, Sivertsson A, Kampf C, Sjostedt E, Asplund A, Olsson I, Edlund K, Lundberg E, Navani S, Szigyarto CA, Odeberg J, Djureinovic D, Takanen JO, Hober S, Alm T, Edqvist PH, Berling H, Tegel H, Mulder J, Rockberg J, Nilsson P, Schwenk JM, Hamsten M, von Feilitzen K, Forsberg M, Persson L, Johansson F, Zwahlen M, von Heijne G, Nielsen J, Ponten F (2015) Proteomics tissue-based map of the human proteome. Science 347:1260419

Veach RA, Liu D, Yao S, Chen Y, Liu XY, Downs S, Hawiger J (2004) Receptor/transporter-independent targeting of functional peptides across the plasma membrane. J Biol Chem 279:11425–11431

Vedadghavami A, Zhang C, Bajpayee AG (2020) Overcoming negatively charged tissue barriers: drug delivery using cationic peptides and proteins. Nano Today 34:100898

Vives E, Brodin P, Lebleu B (1997) A truncated HIV-1 Tat protein basic domain rapidly translocates through the plasma membrane and accumulates in the cell nucleus. J Biol Chem 272:16010–16017

Williams JA, Sans MD, Tashiro M, Schafer C, Bragado MJ, Dabrowski A (2002) Cholecystokinin activates a variety of intracellular signal transduction mechanisms in rodent pancreatic acinar cells. Pharmacol Toxicol 91:297–303

Wu Y, Wang Y, Liu B, Cheng Y, Qian H, Yang H, Li X, Yang G, Zheng X, Shen F (2020) SN50 attenuates alveolar hypercoagulation and fibrinolysis inhibition in acute respiratory distress

syndrome mice through inhibiting NF-kappaB p65 translocation. Respir Res 21:130
Xie J, Bi Y, Zhang H, Dong S, Teng L, Lee RJ, Yang Z (2020) Cell-penetrating peptides in diagnosis and treatment of human diseases: from preclinical research to clinical application. Front Pharmacol 11:697
Yokoo H, Oba M, Uchida S (2021) Cell-penetrating peptides: emerging tools for mRNA delivery. Pharmaceutics 14:78
Yu JH, Kim H (2014) Oxidative stress and inflammatory signaling in cerulein pancreatitis. World J Gastroenterol 20:17324–17329
Zhang L, Torgerson TR, Liu XY, Timmons S, Colosia AD, Hawiger J, Tam JP (1998) Preparation of functionally active cell-permeable peptides by single-step ligation of two peptide modules. Proc Natl Acad Sci U S A 95:9184–9189
Zhu P, Jin L (2018) Cell penetrating peptides: a promising tool for the cellular uptake of macromolecular drugs. Curr Protein Pept Sci 19:211–220